# Reducing uncertainty in characterization of Vaca Muerta Formation Shale with poststack seismic data

Ritesh Kumar Sharma[1], Satinder Chopra[1], Luis Vernengo[2], Eduardo Trinchero[2], and Claudio Sylwan[2]

## Abstract

The Late Jurassic–Early Cretaceous Vaca Muerta (VM) Formation in the Neuquén Basin has served as an important source rock for many of the conventional oil and gas fields in Argentina. With the interest in developing and exploiting shale resources in the country, many companies there have undertaken characterization of the VM Formation in terms of the elements of shale plays. Among other characteristics, shale plays can be identified based on the total-organic-carbon (TOC) content; better TOC leads to better production. However, there is no way of measuring it directly using seismic data, and it can be estimated only indirectly. Considering the influence of TOC on compressional and shear velocities and density, geoscientists have attempted to compute it using the linear or nonlinear relationship it might have with P-impedance. Understanding the uncertainty in using such a relationship for characterizing the VM Formation, a different approach has been followed for characterizing it. Because a linear relationship seems to exist between gamma ray (GR) and TOC, in addition to P-impedance, gamma ray is another parameter of interest for characterizing the VM Formation. Using P-impedance and GR volumes, a Bayesian classification approach has been followed to obtain a reservoir model with different facies based on TOC and the associated uncertainty with it. As the first step, different facies were defined, based on the cutoff values for GR and P-impedance computed from well-log data. Then Gaussian ellipses were used to capture the distribution of data in a crossplot of GR versus P-impedance. Next, 2D probability density functions (PDFs) were created from the ellipses for each of the facies. Combining these PDFs with GR and P-impedance volumes, different facies were identified on the 3D volume. Poststack model-based inversion was used to compute the P-impedance volume, and the probabilistic neural-network (PNN) approach was used to compute GR volume. Derived P-impedance and GR volumes correlated nicely at blind wells on the 3D volume, which gave confidence in the characterization of the VM Formation. An overlay of the discontinuity detail in terms of curvature lineaments on the determined TOC content at the level of interest helps in obtaining a more complete picture, which is useful for the planning of horizontal wells.

## Introduction

The Neuquén Basin in Argentina was developed as a result of an extensional rifting in the Late Jurassic established between a back arc to the west, associated with the Sudamerican (South American) Plate, and a passive margin to the east. Subsequent deposition, thermal subsidence, and structural evolution led to the recognition of five geographic areas (Figure 1) in the basin. They are (1) the thrust-belt area to the west, called the Malargüe-Agrio fold belt, (2) the Northeast Platform, (3) the Embayment in the center, (4) the Huincul Uplift adjoining the Embayment to the south, and (5) the Picún Leufú subbasin to the southwest. All these areas form the elongated northwest-to-southeast shape of the Neuquén Basin, as seen in Figure 1.

Based on the subsurface data from the electrical and acoustic log curves, mud-logging data, and borehole images, extensive facies studies have been carried out in the Neuquén Basin. It has been found that the Vaca Muerta (VM) Formation comprises a variety of lithologies that include organic-rich calcareous shales, marls, carbonates, calcareous sandstones, and sandstones (Fantin et al., 2014; Ortiz Sagasti et al., 2014; Sylwan, 2014).

The present available description of the VM Formation includes the following. It is composed of amorphous organic matter associated with marine plankton and equivalent to Type II or IIS kerogen (Tissot et al., 1974). With regard to thermal maturity, the maximum vitrinite reflectance, $R_o$, varies between 0.8% and

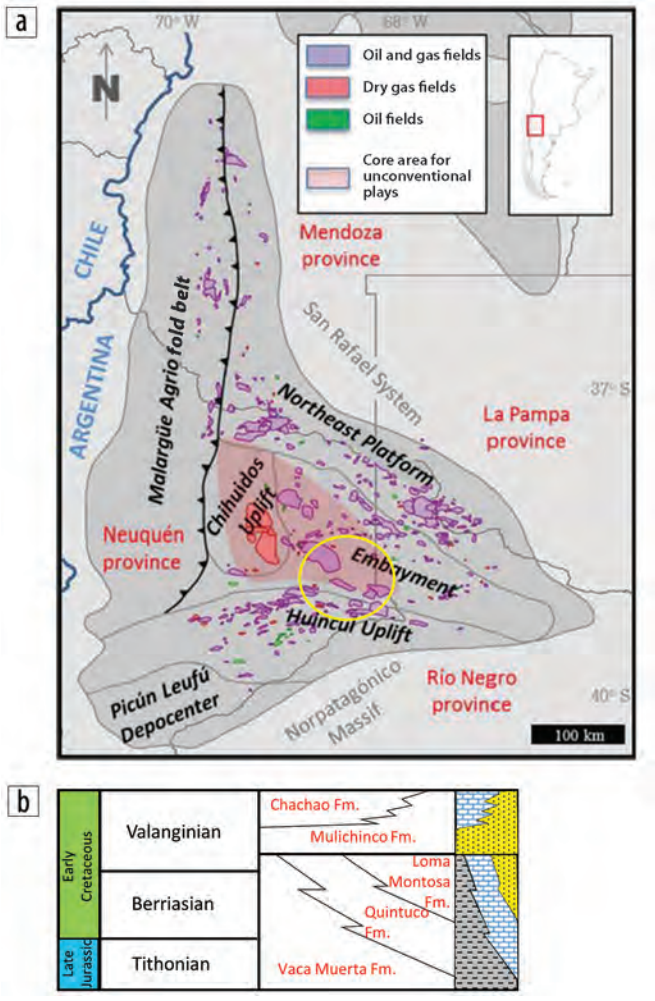


**Figure 1.** Location map and morphostructural features of Neuquén Basin. After Sylwan (2014), Figure 1. Used by permission.

[1]Arcis Seismic Solutions, TGS.
[2]Pan American Energy LLC.

http://dx.doi.org/10.1190/tle34121462.1.

2%. The TOC is 3% to 8% and is found to be higher in the lower parts of the VM Formation (Sylwan, 2014).

As studied by Wavrek et al. (1994), the Embayment area is inhabited by Type A-1 oil, which is light (30° to 45° API) and thermally mature. Similarly, petrophysical analysis on log data shows that porosities vary between 4% and 12% in the VM Formation, with the lower intervals exhibiting porosities of 8% to 12% and the upper intervals 4% to 8% (Di Benedetto et al., 2014).

## Theory and method

For a shale reservoir to become a successful shale resource play, the following characteristics need to be considered: (1) organic richness (TOC), (2) maturation ($R_o$%), (3) thickness, (4) gas in place, (5) permeability, (6) mineralogy, (7) brittleness, and (8) pore pressure. Besides all these, the depth of the shale-gas formation also should be considered because it will have a bearing on the economics of the gas recovery. An optimum combination of these factors leads to favorable productivity (Chopra et al., 2012).

Determination of TOC content allows us to identify the source rocks. Borehole measurements (such as well-log curves) and geochemical analysis and measurements on cores and cuttings are some direct ways of estimating TOC. These methods are applicable only at well locations. However, our goal is to characterize the source rocks not vertically but laterally for deciding on the location of horizontal wells in the area. Thus, seismic data play an important role in identifying sweet spots because they are acquired over large areas.

The determination of TOC content directly from seismic data is a difficult task, but it can be attempted indirectly, as we describe in this study. It is well known that TOC influences compressional velocity, shear velocity, and density of rock intervals. Thus, it should be possible to detect changes in TOC from the seismic response.

In addition, there is evidence of a linear relationship between the uranium content in shale and its organic content. Consequently, a large GR response is expected for organic-rich shale formations. Thus, we should be able to identify source rocks with the help of the GR response.

As mentioned above, P-impedance and GR are two important parameters for identifying the source rocks in terms of TOC. Although P-impedance can be determined by available methods of impedance inversion, there is no direct way of computing GR volume from seismic data. Extended elastic impedance (Whitcombe, 2002) provides a way of computing it from seismic data, but for the case study at hand, the lack of prestack data prevented us from using it.

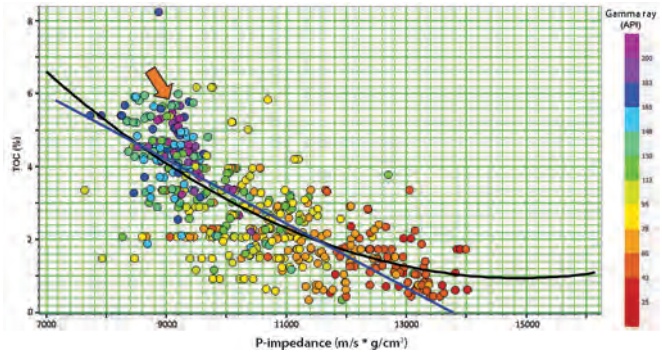


**Figure 2.** Crossplot of measured P-impedance versus TOC color-coded with GR. Best-fit lines showing a linear (blue) and nonlinear (black) relationship are shown. Neither relationship captures the high TOC zones, indicated by the orange arrow.

Because only stacked data was available, a neural-network approach was used for achieving our goal. Neural networks make it possible to predict suitable petrophysical properties such as porosity, GR, water saturation, and so forth away from the well, using a nonlinear relationship between seismic data and different derived attributes with petrophysical properties (Calderon and Castagna, 2007; Singh et al., 2007).

## Characterization of the Vaca Muerta Formation

A feasibility study was conducted for characterizing the VM Formation with the use of stacked seismic data along with available well-log curves and geochemical data. By using the TOC values from geochemical analysis of source-rock cutting samples and the acoustic impedance from well-log data, Løseth et al. (2011) demonstrate that acoustic impedance decreases nonlinearly with increasing TOC percent. This relationship then was used to transform a seismic acoustic-impedance data volume into a TOC volume.

With this in mind and using similar data, we crossplotted P-impedance and TOC to see if any relationship existed between these two attributes. Figure 2 shows this crossplot. It appears that both a linear and a nonlinear curve could be a reasonable fit to the data points (as indicated). However, the important point to note is that whichever relationship is used, the high TOC intervals will remain underestimated in both ways. This is a limitation of the Løseth et al. (2011) approach. Predicting TOC based only on such an approach would have an inherent uncertainty and so was not considered advisable.

Given the fact that the GR response is related to organic richness, it was used to color-code the crossplot. As seen in Figure 2, a better correlation of high GR with high TOC is noticed.

We also crossplotted P-impedance against GR and color-coded it with TOC, as shown in Figure 3a. Because high values of TOC and GR are the characteristics of a better-quality shale play, we enclosed such points on the crossplot with a red polygon and back-projected them to the well-log curves shown in Figure 3b. We notice that most of the points enclosed in the red polygon are from the deeper reservoir zone as expected, suggesting that P-impedance and GR together can be used to differentiate between deeper and shallower part of the reservoir. However, such differentiation would not be possible based on the TOC estimated from the P-impedance using a linear/nonlinear relationship. Even if differentiation were achieved, uncertainty still would exist in terms of quality of the shale.

Because we are attempting to characterize the Vaca Muerta Shale reservoir from seismic data, it is possible that different models that we deduce have the same seismic response. Of course, some of those models will be more probable than others, which we could term as being realistic. Consequently, we followed an approach that accounts for the uncertainties associated with the reservoir characterization of the VM Formation. This work follows the Bayesian classification approach and provides a facies model reflecting the quality of the shale and a related uncertainty analysis.

To execute the Bayesian approach, different facies were defined based on the cutoff values of GR and P-impedance. Armed with this facies information, the probability distribution functions

(PDFs) were generated for them using Gaussian ellipses. Figure 4 shows these ellipses, where three facies are defined in green (facies 1), dark green (facies 2), and red (facies 3). Based on the P-impedance and GR values, the quality of shale play must increase from red to green. Observing the defined facies on the well-log panel, it was concluded that the quality of the VM Formation increases with depth, which is reasonable based on the known geologic history.

Having gained confidence in characterizing the VM Formation based on well-log curves, we turned to deriving the seismic P-impedance and GR volumes. For computing P-impedance, stacked seismic data first were conditioned in terms of enhancing the signal-to-noise ratio (S/N). A low-frequency model was created using five of the eight wells, keeping the other three as blind wells.

After observing a good correlation at the blind wells, model-based inversion was used to invert the seismic data. Routine quality checks included inversion analysis at well locations, overlay of acoustic-impedance logs (filtered to the seismic bandwidth) on acoustic-impedance sections, and crossplotting the predicted and actual acoustic-impedance values at well locations.

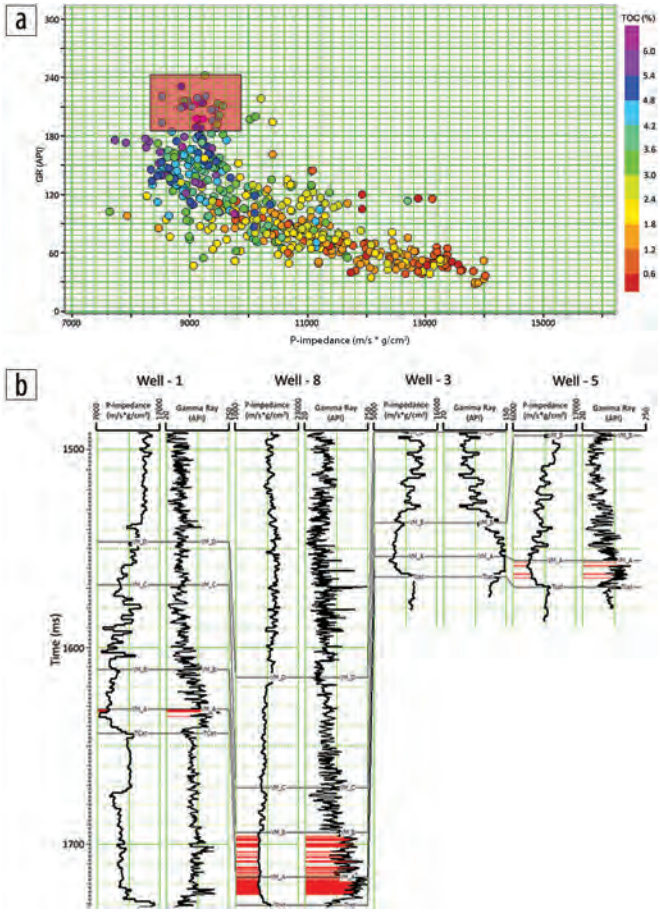


**Figure 3.** (a) Crossplot of measured P-impedance versus GR color-coded with TOC. A relationship is noticed between high TOC and high GR and P-impedance. Points with high values of both are captured as shown with the red polygon and are back-projected to the well-log curves, as shown in part (b). These points are seen to come from the deeper reservoir zone, as expected. Thus a crossplot of P-impedance with GR allows us to differentiate between deeper and shallower part of the reservoir.

When we found all these results encouraging, we proceeded with the inversion of the complete volume. Two portions of an arbitrary profile passing through the wells were extracted from the inverted impedance volume and are shown in Figure 5. A good match between inverted and measured impedance was found at each of the well locations, which provided confidence in the inversion process used. (Figure 12 shows the complete path of the arbitrary line.)

For computing the GR volume, multiattribute regression and the probabilistic neural network (PNN) were used. The detailed theory and workflow on PNN can be found in Hampson et al. (2001). The different steps followed were first multilinear regression

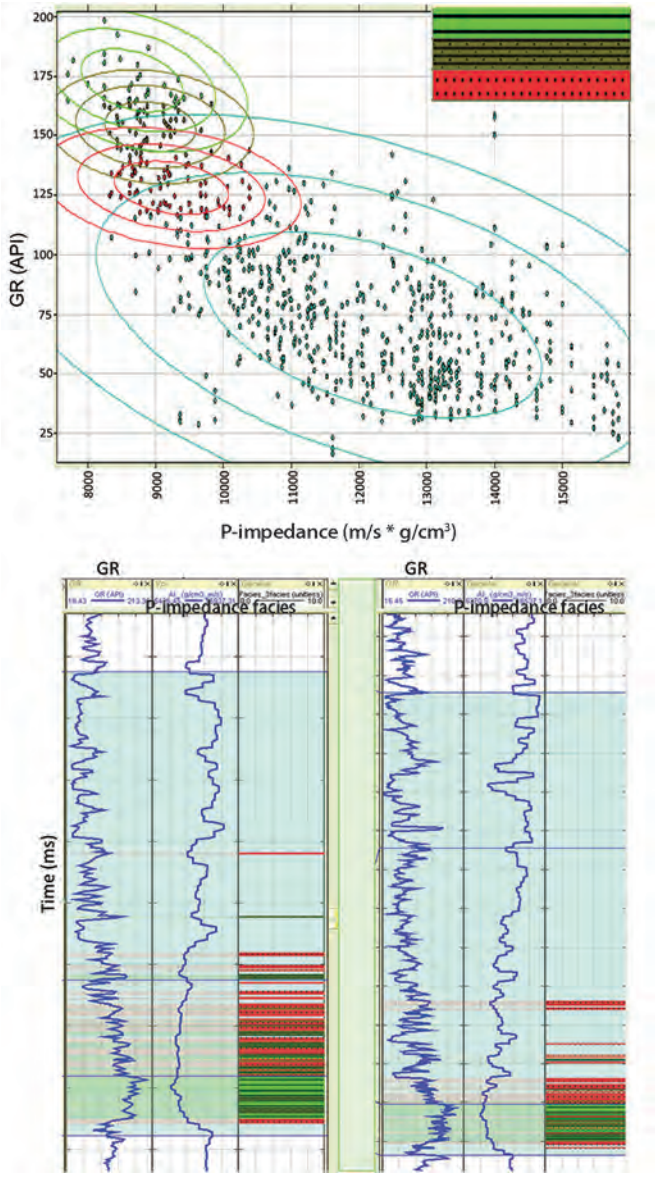


**Figure 4.** Based on the cutoff values of GR, three facies were defined and are shown here in light green, dark green, and red on the crossplot of P-impedance versus gamma ray. Observing the defined facies on the well-log panel (obtained after projection from the crossplot), it can be concluded that the quality of the Vaca Muerta Formation increases with depth, which is trustworthy based on the known geologic history. Gaussian ellipses shown here were used for creating probability density functions of each facies and carrying out the subsequent uncertainty analysis.

analysis followed by selection of optimized parameters and attributes using cross-validation criteria. Next, training of PNN networks was carried through, and finally, the trained PNN network was run on the selected seismic attributes for prediction of the desired property.

The multilinear regression analysis run on seismically derivable attributes was performed using eight wells. (Figure 10 shows the location of the wells.) The convolution operator length and optimum number of attributes were chosen using cross-validation criteria (Hampson et al., 2001). Although the additional attributes always improve the fit to the training data, they might be useless or worse when applied to new data not in the training set. This is sometimes called overtraining. In cross-validation, one well at a time is excluded from the training data set, and prediction error is calculated at the location of the blind well. The analysis is repeated as many times as there are wells, each time leaving out a different well.

An operator length of nine samples gave the minimum validation error with five attributes. The attributes were 1/(P-impedance), average frequency, integrated absolute amplitude, filter of (25/30–35/40), and filter of (5/10–15/20) on seismic data. By performing the stepwise regression and validation tests before training the PNN, the problem of overfitting the data is eliminated.

Figure 6 shows the crossplot of the actual and predicted GR response at different well locations, where a correlation of 95% is seen. Figure 7 shows validation correlation between actual and predicted GR logs (over a zone bounded by blue bars), and again, good correlation is seen.

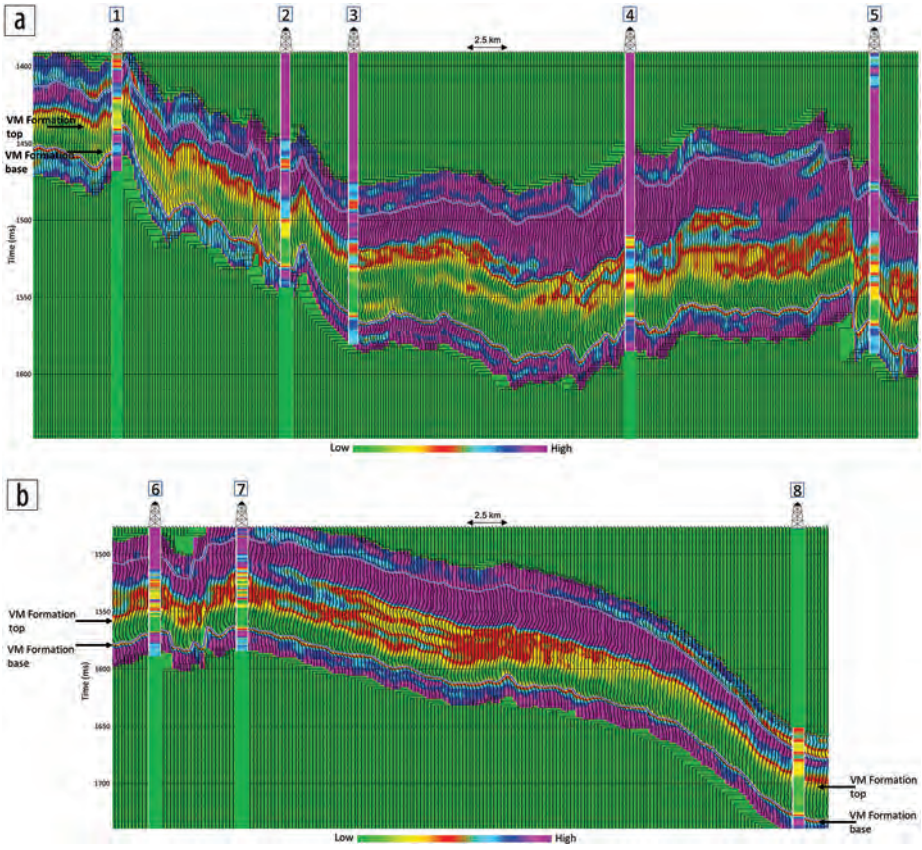


**Figure 5.** Inverted P-impedance section along an arbitrary line that passes through the Wells and is shown in Figure 10. Part of the line passing through wells 1 through 5 is shown in part (a), and the other part passing through Wells 6 to 8 is shown in part (b). A reasonably good correlation is noticed between inverted and measured impedances.

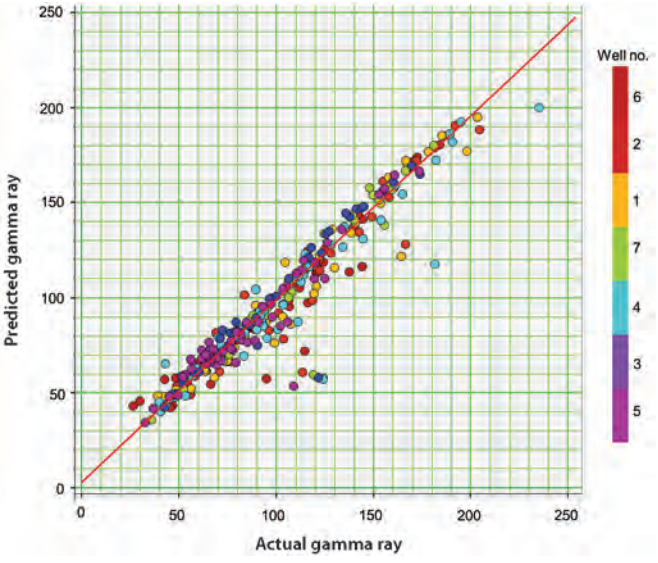


**Figure 6.** Crossplot of actual and predicted GR response using the PNN approach on five seismic attributes. A correlation of 95% is noticed.

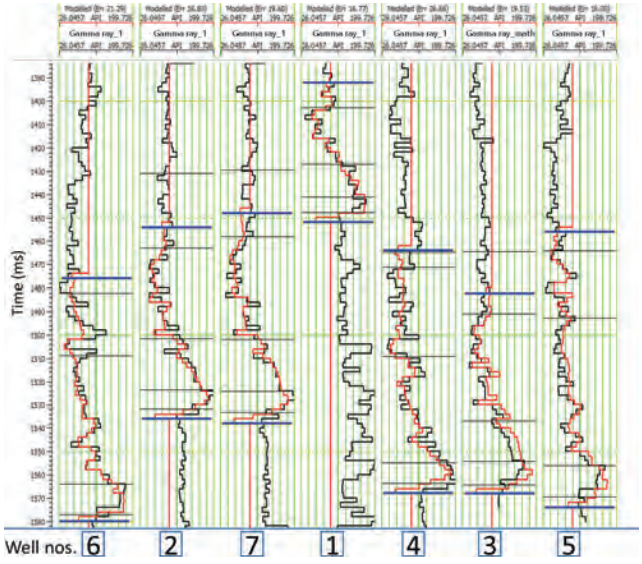


**Figure 7.** Log panel showing the match between actual (black) and modeled (red) GR log curves derived using PNN for different wells after validation.

Regarding the five attributes used in the analysis, one notices the dominance of the frequency-dependent attributes that is biased on the low-frequency side and might wonder about the rationale for their application. We believe the low-frequency dominance in the broad zone of interest is associated with the presence of fractures and the hydrocarbons in the reservoir. Their combination with the 1/(P-impedance) attribute makes lithology prediction become feasible.

Using the probability distribution function of each facies generated earlier from well-log data analysis and inverted P-impedance and GR volumes, Bayesian classification generated the facies volume and probability volume of each facies.

Figure 8 shows an arbitrary line extracted from the facies volume and passing through three wells (which have TOC measurements from cores). We find that the quality of the shale reservoir is better in the lower part of the VM Formation, and the thickness of facies 1 (green) increases from the shallower part to the deeper part of the interval, as expected from the geologic information.

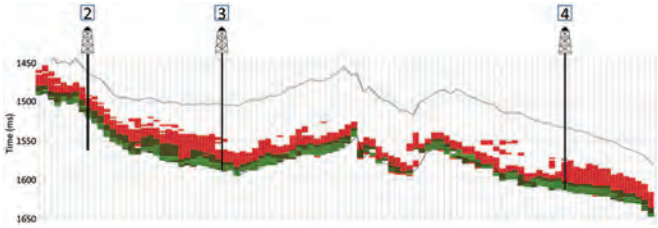


**Figure 8.** Arbitrary line extracted from the facies volume and passing through three wells. The better quality of the shale reservoir is noticed in the lower part of the Vaca Muerta Formation. The thickness of facies 1 (green) increases from the shallower to the deeper part of the interval, as expected from the geologic information. The segment of the profile displayed is indicated in Figures 10 and 11.

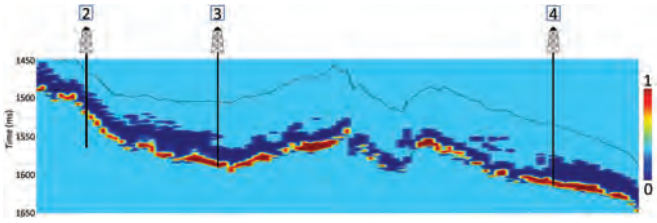


**Figure 9.** Arbitrary line extracted from the probability volume for facies 1. The high probability of occurrence of this facies is represented by brown. The segment of the profile displayed is indicated in Figures 10 and 11.

Figure 9 shows a similar section extracted from the probability volume for facies 1. The color scheme represents the probability of this facies, with brown representing a higher probability of occurrence of facies 1.

In a similar way, the probability distribution of other facies can be extracted. For detecting the probable sweet spots, horizon slices were extracted from the facies volume at different levels. Figure 10 shows one such horizon slice extracted 8 ms above the base of the reservoir, where facies 1 seems to dominate the display.

Finally, in Figure 11, we show a map depicting the probability of occurrence of facies 1. Hot colors indicate zones where the probability of occurrence of facies 1 is 85% and higher. Because facies 1 corresponds to high TOC, these zones were treated as sweet spots. This map correlated nicely at the well locations in this interval, which enhanced our confidence in the results. Similar analyses were carried out for other intervals that exhibit different facies.

For the purpose of comparison of our workflow with the Løseth et al. (2011) approach, the P-impedance volume was transformed using the nonlinear trend shown in Figure 2.

Figure 12 shows a horizon slice 8 ms above the base of the reservoir. Notice that the distribution of hot colors showing favorable pockets on the TOC display is different from the sweet spots determined by using the proposed workflow. Overlaid on the TOC display is the most-positive-curvature attribute, using a transparency. Although the seismic signature of some of the bigger and more coherent lineaments (marked with magenta arrows) confirms them as faults, many of the consistent and weaker lineaments (indicated with orange arrows) have been interpreted as eolian events associated with megadunes (Cardoso et al., 2012; Trinchero et al., 2013).

The characteristics of the sedimentary events that deposited the basal part of the Vaca Muerta sequence have been studied based on the geology of the area and the well data. These events are not conspicuous on seismic amplitudes but can be detected easily on curvature attribute displays. A clear distinction between such events and lineaments with other orientations therefore can be made on the display shown in Figure 12. Lineaments with

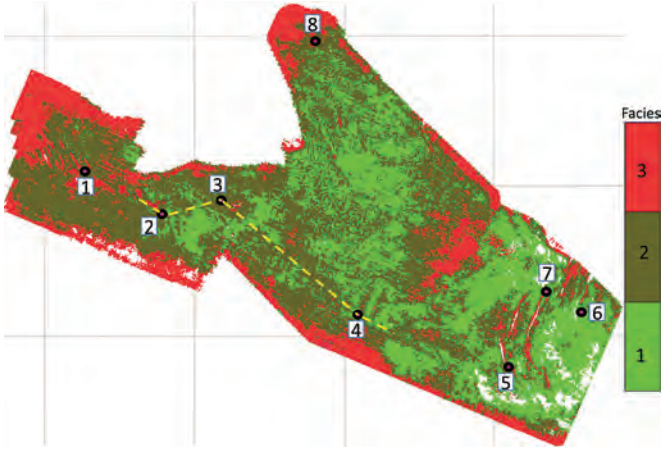


**Figure 10.** Distribution of different facies along a horizon slice taken 8 ms above the base of the reservoir. Facies 1 seems to dominate the display.

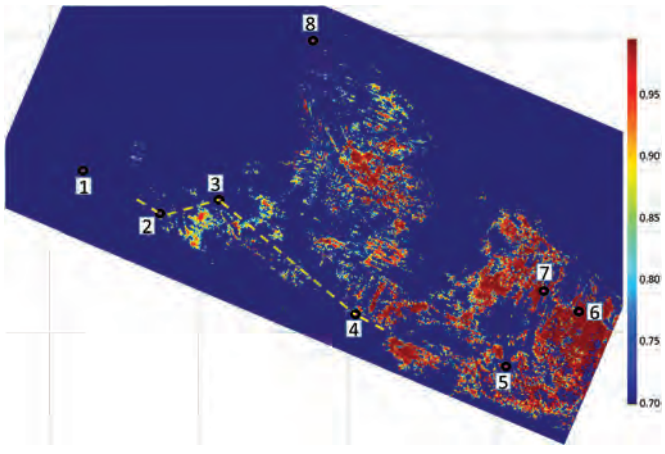


**Figure 11.** Map depicting the probability of occurrence of facies 1. The hot colors on this map indicate zones where the probability of occurrence of the high TOC zone is greater than 85%.

other orientations could be associated with faults and fractures and could be confirmed by image logs available in the area. Such lineaments should be considered carefully while deciding on the location of horizontal wells to be drilled in the VM Formation.

## Conclusions

Determination of TOC in shale-resource reservoirs is a desirable goal in most projects carried out for characterization of unconventional reservoirs. TOC calculations based on linear or nonlinear relationships between acoustic impedance from log data and TOC values could lead to uncertainty and were not found suitable for use in characterization of the Vaca Muerta Formation. The application of poststack model-based P-impedance and GR volume derived using PNN, coupled with a Bayesian classification approach, provided a useful workflow for defining different facies in the VM Formation and hence the quality of the shale. This workflow has the potential of good application to other shale plays around the world. TLE


## Acknowledgments

We thank Arcis Seismic Solutions, TGS, and Pan American Energy LLC for allowing us to present this work.



Corresponding author: SChopra@arcis.com


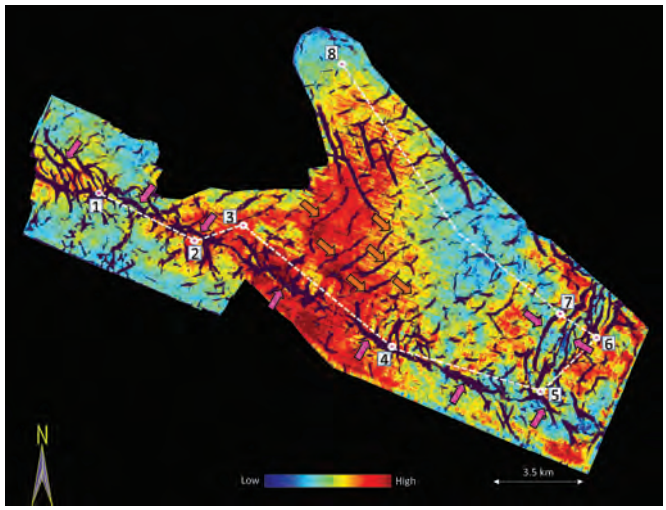


**Figure 12.** Horizon slice from the TOC volume 8 ms above the base of the reservoir. Notice that the distribution of TOC pockets is different from the sweet spots determined by using the Bayesian workflow. Overlaid on the TOC display is the most-positive-curvature attribute, using a transparency. Lineaments in black have been interpreted as eolian events associated with megadunes (orange arrows) and faults (magenta arrows) and fractures in the zone of interest.

## References


Calderon, J. E., and J. P. Castagna, 2007, Porosity and lithology estimation using rock physics and multi-attribute transforms in Balcon field, Colombia: The Leading Edge, **26**, no. 2, 142–150, http://dx.doi.org/10.1190/1.2542439.

Cardoso, J., E. Trinchero, and L. Vernengo, 2012, A seismic characterization of a non-conventional reservoir using geometric and geomechanical attributes: V Simpósio Brasileiro de Geofísica (VSBGf), Actas, November, 1–6.

Chopra, S., R. K. Sharma, J. Keay, and K. J. Marfurt, 2012, Shale gas reservoir characterization workflows: 82nd Annual International Meeting, SEG, Expanded Abstracts, http://dx.doi.org/10.1190/segam2012-1344.1.

Di Benedetto, M., P. Biscayart, J. Zunino, and J. Soldo, 2014, Geological setting of the Vaca Muerta Formation, Neuquén Basin — A world class shale play: 76th Conference and Exhibition, EAGE, Extended Abstracts, WS7-A01, http://dx.doi.org/10.3997/2214-4609.20140541.

Fantin, M., L. Crousse, S. Cuervo, D. Vallejo, F. Gonzalez Tomassini, H. Reijenstein, and C. Lipinski, 2014, Vaca Muerta stratigraphy in central Neuquén Basin: Impact on emergent unconventional project: Unconventional Resources Technology Conference (URTeC), 2741–2751, http://dx.doi.org/10.15530/urtec-2014-1923793.

Hampson, D. P., J. S. Schuelke, and J. A. Quirein, 2001, Use of multi-attribute transforms to predict log properties from seismic data: Geophysics, **66**, no. 1, 220–236, http://dx.doi.org/10.1190/1.1444899.

Løseth, H., L. Wensaas, M. Gading, K. Duffaut, and M. Springer, 2011, Can hydrocarbon source rocks be identified on seismic data?: Geology, **39**, no. 12, 1167–1170, http://dx.doi.org/10.1130/G32328.1.

Ortiz Sagasti, G. A., D. Hryb, M. Foster, and V. Lazzari, 2014, Understanding geological heterogeneity to customize field development: An example from the Vaca Muerta unconventional play, Argentina: Unconventional Resources Technology Conference (URTeC), 797–816, http://dx.doi.org/10.15530/urtec-2014-1923357.

Singh, V., A. K. Srivastava, D. N. Tiwary, P. K. Painuly, and M. Chandra, 2007, Neural networks and their applications in lithostratigraphic interpretation of seismic data for reservoir characterization: The Leading Edge, **26**, no. 10, 1244–1260, http://dx.doi.org/10.1190/1.2794381.

Sylwan, C., 2014, Source rock properties of Vaca Muerta Formation, Neuquina Basin, Argentina: Presented at the IX Congreso de Exploración y Desarrollo de Hidrocarburos: Simposio de Recursos No Convencionales: Ampliando el Horizonte Energético, 365–386.

Tissot, B. P., B. Durand, J. Espitalié, and A. Combaz, 1974, Influence of nature and diagenesis of organic matter in formation of petroleum: AAPG Bulletin, **58**, no. 3, 499–506.

Trinchero, E., L. Vernengo, and J. Cardoso, 2013, Geomechanical and geometric seismic attributes in an interpretation workflow for characterization of unconventional reservoirs: The Leading Edge, **32**, no. 4, 386–392, http://dx.doi.org/10.1190/tle32040386.1.

Wavrek, D. A., M. E. Lara, J. C. Quick, J. W. Collister, and R. B. Allen, 1994, Neuquén Basin, Argentina: An integrated geochemical study, 4: Integrated basin analysis: Earth Science and Resources Institute, University of South Carolina, ESRI Technical Report 94-08-422.

Whitcombe, D. N., 2002, Elastic impedance normalization: Geophysics, **67**, no. 1, 60–62, http://dx.doi.org/10.1190/1.1451331.